Histol Histopathol (2023) 38: 453-465

http://www.hh.um.es

Histology and Histopathology
From Cell Biology to Tissue Engineering

ORIGINAL ARTICLE **Open Access**

The clinicopathological and prognostic significances of CDC73 expression in breast cancer: A pathological and bioinformatics analysis

Ying E[1], Hang Xue[1], Cong-Yu Zhang[2], Ming-Zhen Zhao[3] and Hua-Chuan Zheng[1]

[1]Department of Oncology and Center Laboratory, The Affiliated Hospital of Chengde Medical University, Chengde, China,

[2]Cancer Center, The First Affiliated Hospital of Jinzhou Medical University, Jinzhou, China and

[3]Department of Respiratory Medicine, The Affiliated Hospital of Chengde Medical University, Chengde, China

Summary. Parafibromin is a protein encoded by the oncosuppressor CDC73 gene, whose mutation results in hyperparathyroidism-jaw tumor syndrome (HPT-JT) and parathyroid carcinoma. Down-regulation of parafibromin is linked to lung, gastric, colorectal, and ovarian cancer tumorigenesis. Parafibromin expression was detected by RT-PCR, bioinformatics analysis, Western blot, and immunohistochemistry; and compared with clinicopathological characteristics of breast cancer. CDC73-related genes and pathways were analyzed using bioinformatics analysis. Parafibromin expression was increased in breast cancer compared to normal tissues at both mRNA and protein levels ($p<0.05$). Among triple-negative breast cancers, it was higher in basal-like 1 than basal-like 2 patients ($p<0.05$) and mesenchymal than immunomodulatory patients ($p<0.05$). CDC73 mRNA expression was positively correlated with white race, non-infiltrating immune cells, favorable luminal subtypes of PAM50, and prognosis of breast cancer patients ($p<0.05$). The differential genes of CDC73 were classified into enzyme inhibitors, peptidase, and keratinization by KEGG ($p<0.05$). Similarly, it was classified into ribosomes, TGF-β, oxidation phosphorylation, inositol phosphate metabolism, arachidonic acid metabolism, linoleic acid metabolism, ERBB, and VEGF signaling pathways by GSEA ($p<0.05$). The positively-correlated genes of CDC73 were involved in cell mobility, response to interferon α, nuclear pore and basket, and histone methyltransferase. The negatively-correlated genes of CDC73 were involved in the mitochondrial respiratory chain, thermogenesis, and ribosomes. Parafibromin expression was higher in invasive ductal than lobular carcinoma ($p<0.05$) and mucinous adenocarcinoma than others ($p<0.05$). Parafibromin immunoreactivity as an independent factor was positively associated with an increased overall survival rate of breast cancer patients ($p<0.05$). These findings suggest that up-regulation of parafibromin in breast cancer patients is closely linked to a favorable prognosis. It is involved in tumorigenesis and subsequent progression by regulating metabolism, ribosomes, and cytokines.

Key words: Breast cancer, Prognosis, Parafibromin, Pathobiological behaviors

Corresponding Author: Hua-chuan Zheng, Department of Oncology and Center Laboratory, The Affiliated Hospital of Chengde Medical University, Chengde 067000, PR China. email: zheng_huachuan@hotmail.com

DOI: 10.14670/HH-18-534

Introduction

Breast cancer (BC) is the most commonly diagnosed cancer in women worldwide, and its morbidity and mortality rates have increased rapidly. The risk factors of BC include age at first menarche, age at first pregnancy, age at menopause, high estradiol exposure, mental stress, obesity, coffee consumption, radiation exposure, family history of BC, and germline mutations, deletion, and insertion. Based on genetic analysis, BC can be divided into Luminal A, Luminal B, HER2-positive, and basal-like subtypes (Rojas and Stuckey, 2016; Coughlin, 2019). Therefore, it is essential to identify novel biomarkers for the diagnosis, treatment, and prevention of BC.

As an oncosuppressor, parafibromin is a protein encoded by the *CDC73*, whose mutation leads to hyperparathyroidism-jaw tumor syndrome (HPT-JT) and parathyroid cancer (PC) (Aldred et al., 2006). In the nucleus, parafibromin protein can be involved in the formation of the polymerase-associated factor (PAF) 1 complex, which inhibits RNA polymerase II-mediated transcription of c-Myc, Cyclin D1, and β-catenin. It is also involved in histone H2B ubiquitination, histone H3 methylation, poly-A elongation, and post-transcriptional

modifications (Lin et al., 2008; Kikuchi et al., 2016). Nene et al. reported that parafibromin suppresses genome instability by mediating telomere homeostasis and repairing chromosomal rearrangements(Nene et al., 2018). Parafibromin might associate with the ring finger proteins (RNF) 20 and 40 to ubiquitinate histone 2B (Hahn et al., 2012). Parafibromin expression was found to arrest G_1 by suppressing Cyclin D1 *via* H3K9 methylation (Yang et al., 2010). In contrast, parafibromin could function as an oncogene by interacting with β-catenin to initiate the Wnt/β-catenin signaling pathway following tyrosine dephosphorylation by SHP2 (Takahashi et al., 2011). In the cytoplasm, parafibromin induces apoptosis by activating Caspase-9 and -3 and down-regulating Survivin and bcl-2 expression (Zhu et al., 2016). Upon IFM- γ stimulation, parafibromin expression promotes the formation of the JAK1/2 - STAT1 complex, which induces STAT1 phosphorylation at Tyr701 (Wei et al., 2015). Parafibromin interacts with muscle α-actinin 2/4 to promote mobility (Agarwal et al., 2008). This finding is supported by parafibromin immunopositivity in the cilia of the bronchial pseudo-stratified columnar ciliated epithelium (Xia et al., 2011) and fallopian tube (Shen et al., 2016).

Walls et al. found that mice with parathyroid-specific deletion of *Cdc73* developed uterine and parathyroid tumors (Walls et al., 2017). This model might be employed as an animal model for HPT-JT syndrome. Witteveen et al. found that the loss of parafibromin was found in 13 of 23 PC patients and was associated with a 4-fold increased risk of developing local or distant metastasis (Witteveen et al., 2011). Zhu et al. analyzed 193 PC patients from 9 studies and found that parafibromin immunonegativity is a risk factor for recurrence, metastasis, and death (Zhu et al., 2020). Pyo et al. performed a meta-analysis and found that parafibromin loss was significantly higher in PC than atypical parathyroid adenoma, adenoma, and hyperplasia (Pyo and Cho, 2019). In our previous studies, parafibromin hypoexpression positively correlated with pathogenesis, invasive activity and adverse prognosis of ovarian (Agarwal et al., 2008), lung (Shen et al., 2016), gastric (Zheng et al., 2008), colorectal (Zheng et al., 2011), and head and neck (Zhang et al., 2015) cancers. In the present study, we analyzed the clinicopathological and prognostic significances of CDC73 expression in breast cancer and identified CDC73-related genes and pathways in BC.

Materials and methods

Subjects

Surgical samples of breast cancer tumors (n=658), matched non-neoplastic mucosa (n=110), and metastatic cancer in lymph nodes (n=81) were collected at The First Affiliated Hospital of Jinzhou Medical University between 2010 and 2020. Among them, 280 cases had lymph node metastasis. Additionally, 76 cases of frozen breast cancer and paired normal tissues were collected for RNA and protein analysis. None of the patients received radiochemotherapy or other adjuvant treatment before surgery. Informed consent to use cancer tissues for scientific research was obtained from patients or their relatives. The ethical committee at The Affiliated Hospital of Chengde Medical University approved the research protocol.

RNA extraction and RT-PCR

Total RNA was isolated from breast cancer and normal tissues using Trizol (Takara). Complementary DNA was prepared from RNA (2 μg) using random primers and AMV reverse transcriptase. The primers were 5'- CACGAATTGAGGATGAAGAGTG-3' and 5'- CTGTTCAGTCT GTACAATCCCT-3' (95bp) for *CDC73* and 5'-CAATGACCCCTTCATTGACC-3' and 5'-TGGAAGA TGGTGATGGGATT-3' (135 bp) for *GAPDH*. Quantitative PCR was carried out using SYBR Premix Ex Taq II kit (Takara) with *GAPDH* as an internal control. *CDC73* mRNA expression levels in the samples were calculated using the $2^{-\Delta\Delta CT}$ method and normalized to normal tissue.

Western blot

Total protein was isolated from breast cancer and normal tissues using RIPA lysis buffer and subjected to protein quantification. The denatured protein was separated on a 10% SDS-PAGE gel and transferred to a PVDF membrane. Afterward, the membrane was blocked in 5% milk in TBST at room temperature for 30 min. For immunoblotting, the membrane was incubated with mouse anti-parafibromin antibody (Santa Cruz) at room temperature for 60 min, rinsed with TBST, and incubated with IgG conjugated to HRP (DAKO, USA) at room temperature for 60 min. Bands were detected by ECL Western Blotting Substrate (Santa Cruz). Analysis was conducted using Image J, and GAPDH (Sigma) served as control.

Tissue microarray and immunohistochemistry

All pathological blocks were subjected to tissue microarray (TMA). TMA blocks were incised into 4μm-thick sections. The immunohistochemistry was performed as previously described, using mouse anti-parafibromin (Santa Cruz) or rabbit anti-ki-67 (DAKO) antibody (Shen et al., 2016). Immunoreactivity to parafibromin or ki-67 or ER or PR was localized in the nucleus. The positive rate classifications were as follows: 0=0%; 1=1-49%; 2=50-74%; 3≥75%. The positive intensity classifications were as follows: 1=weak; 2=medium; 3=strong. The immunohistochemical score was calculated as the intensity × positive rate, with the scores defined as follows: -=0; +=1-2; ++=3-5; +++=6-9. Immunoreactivity to HER-2 was

localized on the membrane. Interpretation criteria for HER-2 (according to each section) 0: no staining or ≤10% of infiltrating cancer cells showed incomplete, weak cell membrane staining; 1+: >10% of infiltrating cells showed incomplete, weak staining 2+: There are 2 cases, the first is that >10% of the infiltrating cancer cells show weak-moderate intensity of intact cell membrane staining; the second is that ≤10% of the infiltrating cancer cells show strong and intact cell membrane Staining; 3+: >10% of infiltrating cancer cells showed strong, intact and uniform cell membrane staining. For the analysis, 100 cells were randomly chosen and counted from five representative fields by two independent researchers (EY and ZHC).

Bioinformatics analysis

The clinicopathological and prognostic significances

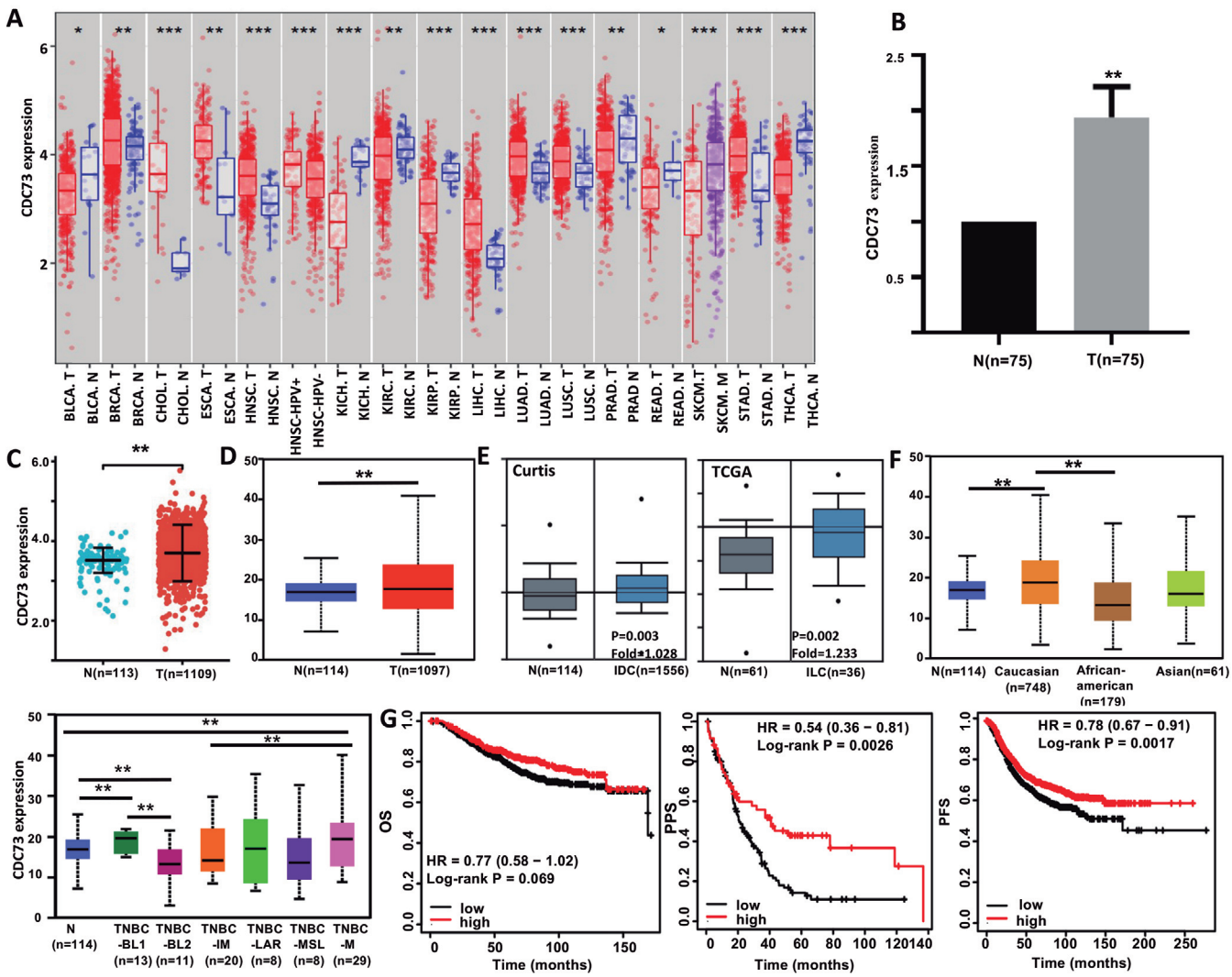

Fig. 1. The clinicopathological significance of CDC73 mRNA expression in breast cancer. The expression profile of CDC73 mRNA was analyzed in various cancers using the Time database **(A)**. CDC73 mRNA expression was significantly higher in breast cancer than in normal tissues, as determined by real-time RT-PCR **(B)**. These results were in agreement with the results from Xiantao **(C)**, UALCAN **(D)**, and Oncomine's **(E)** databases. It was also compared to clinicopathological characteristics of breast cancer using the ULCAN database **(F)**. Kaplan-Meier plotter was employed to analyze the prognostic significance of CDC73 mRNA in breast cancer **(G)**. N, normal mucosa; T, cancer; M, metastasis; IDC, intraductal carcinoma; ILC, intralobular carcinoma; BLCA, bladder urothelial carcinoma; BRCA, breast invasive carcinoma; CHOL, cholangiocarcinoma; ESCA, esophageal adenocarcinoma; HNSC, head and neck squamous cell carcinoma; HPV, human papillary virus; KICH, kidney chromophobe; KIRP, kidney renal clear cell carcinoma; LIHC, liver hepatocellular carcinoma; LUAD, lung adenocarcinoma; LUSC, lung squamous cell carcinoma; PRAD, prostate adenocarcinoma; READ, rectal adenocarcinoma; SKCM, skin cutaneous melanoma; STAD, stomach adenocarcinoma; THCA, thyroid carcinoma; TNBC, triple-negative breast cancer; BL, basal-like; M, mesenchymal; MSL, mesenchymal stem-like; IM, immunomodulatory; LAR, luminal androgen receptor. ***, p<0.01; **, p<0.01;*p<0.05.

of *CDC73* expression in BC were analyzed using the Timer (https://cistrome.shinyapps.io/timer/), UALCAN (http://ualcan.path.uab.edu/), Oncomine (www.oncomine.org) and Xiantao platforms (https://www.xiantao.love/). *CDC73* promoter methylation was also compared with tumorigenesis and clinicopathological characteristics of BC using UALCAN. The correlation between *CDC73* expression and immune cell infiltration was investigated using Xiantao. The differential genes were subjected to the construction of protein-protein interaction (PPI) networks, and important hub genes were selected. These genes were subjected to CC (cellular components) + KEGG and GSEA analysis to construct signaling pathways.

Statistical analysis

Spearman correlation analysis was conducted to compare the rank counting data, and a student's t-test was used to differentiate the means of the two groups. Kaplan-Meier plots and log-rank statistics were used to compare survival curves. We employed Cox's proportional hazards regression model to conduct a multivariate survival analysis. All data were analyzed using SPSS 10.0. $p<0.05$ was regarded as statistically significant.

Results

The correlation of CDC73 mRNA expression with carcinogenesis and pathology of breast cancer

According to Timer, we found that *CDC73* mRNA levels were decreased in bladder cancer, kidney chromophobe, renal clear cell carcinoma, renal papillary cell carcinoma, prostate adenocarcinoma, rectal adenocarcinoma, and thyroid carcinoma compared to normal tissues ($p<0.05$, Fig. 1A). The converse was true for invasive breast carcinoma, cholangiocarcinoma, esophageal adenocarcinoma, head and neck squamous cell carcinoma (HNSCC), hepatocellular carcinoma, lung adenocarcinoma and squamous cell carcinoma, and gastric adenocarcinoma compared to normal tissues ($p<0.05$, Fig. 1A). *CDC73* mRNA expression is positively associated with human papillomavirus (HPV)-related HNSCC and metastasis of cutaneous skin melanoma (Fig. 1A, $p<0.05$). Overexpression of *CDC73* mRNA in breast cancer was verified by RT-PCR (Fig.

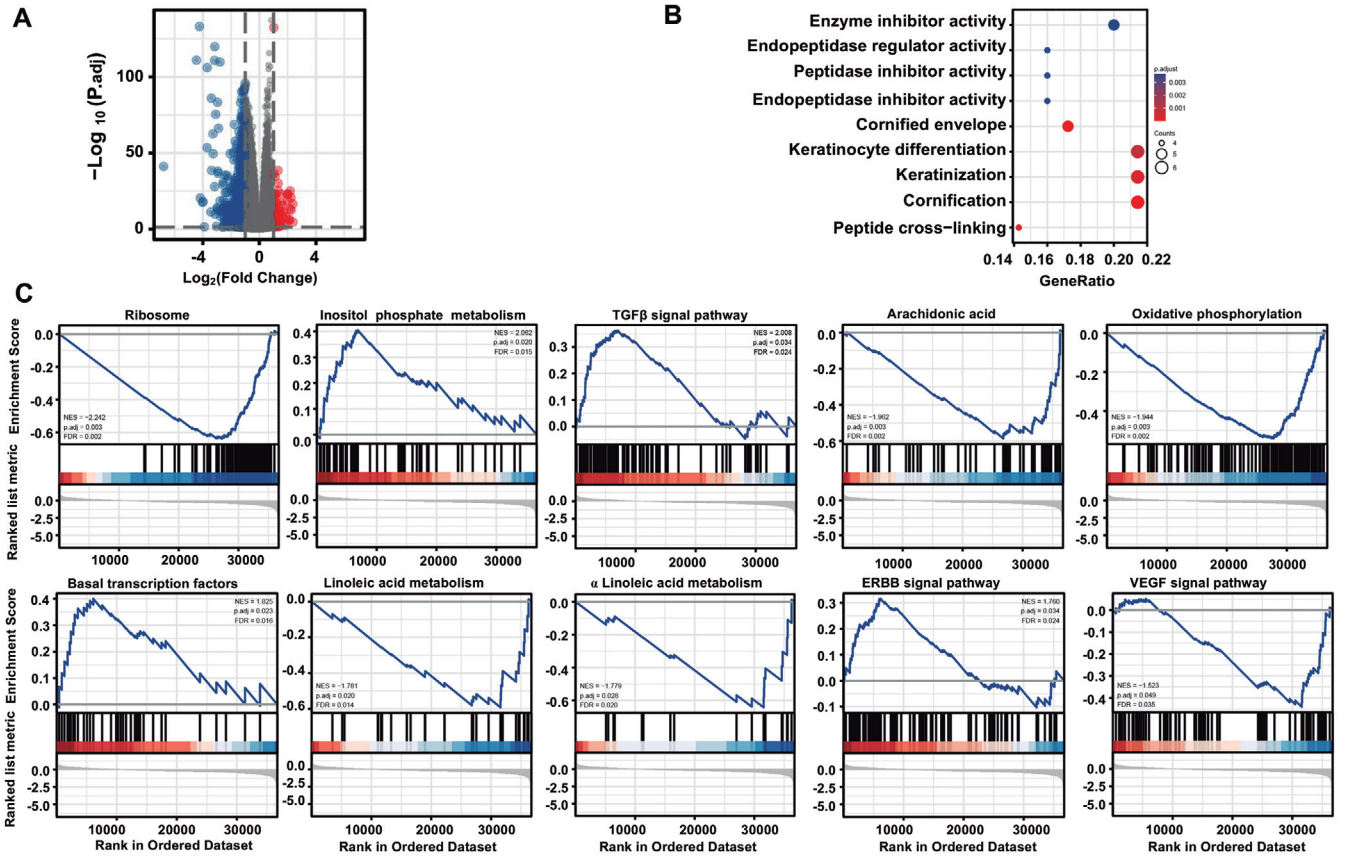

Fig. 2. The differential genes and related signaling pathways involving CDC73 expression in breast cancer. The volcano map of the differential genes of CDC73 is shown in breast cancer **(A)**. These genes were subjected to signaling pathway analysis using KEGG **(B)** and GSEA **(C)**.

1B, p<0.05), Xiantao (Fig. 1C, p<0.05), UALCAN (Fig. 1D, p<0.05), and Oncomine (Curtis's and TCGA's studies) databases (p<0.05, Fig. 1E). As shown in Fig. 1F, *CDC73* was higher in Caucasian than Asian cancer patients (p<0.05), triple-negative breast cancer (TNBC)-BL1 than -BL2 patients (p<0.05), and TNBC-M than -IM patients (p<0.05). As summarized in Table 1, *CDC73* mRNA expression positively correlated with white race and favorable luminal subtypes of PAM50 in BC patients (p<0.05). CDC73 mRNA expression positively correlated with high overall (OS), post-progression (PPS), and progression-free (PFS) survival rates of all the cancer patients according to the Kaplan-Meier plotter (Fig. 1G, p<0.05).

Based on the Xiantao platform (Table 2), we found that CDC73 mRNA expression is negatively correlated to the infiltration of activated dendritic cells, B cells, CD8+ cells, cytotoxic cells, plasma dendritic cells, dendritic cells, interdigitating dendritic cells, mast cells, neutrophils, NK CD56^{bright} cells, NK CD56^{dim} cells, NK cells, T cells, T helper cell, central memory T cell, follicular helper T cell, TGD, Th1 cells, Th17 cells, Th2 cells, and Treg cells in breast cancer (Table 2, p<0.05).

Table 1. The relationship between CDC73 mRNA expression and clinicopathological features of breast cancer.

Clinicopathological features/ Grouping	Low expression	High expression	P
Age, n (%)			
≤60	300 (27.7%)	301 (27.8%)	1.000
>60	241 (22.3%)	241 (22.3%)	
Race, n (%)			
Asian	35 (3.5%)	25 (2.5%)	<0.001
Black or African American	121 (12.2%)	60 (6%)	
White	353 (35.5%)	400 (40.2%)	
T stage, n (%)			
T1	149 (13.8%)	128 (11.9%)	0.188
T2	298 (27.6%)	331 (30.6%)	
T3	76 (7%)	63 (5.8%)	
T4	16 (1.5%)	19 (1.8%)	
N stage, n (%)			
N0	244 (22.9%)	270 (25.4%)	0.451
N1	182 (17.1%)	176 (16.5%)	
N2	58 (5.5%)	58 (5.5%)	
N3	43 (4%)	33 (3.1%)	
M stage, n (%)			
M0	430 (46.6%)	472 (51.2%)	0.673
M1	11 (1.2%)	9 (1%)	
Pathological stage, n (%)			
Stage I	96 (9.1%)	85 (8%)	0.419
Stage II	297 (28%)	322 (30.4%)	
Stage III	125 (11.8%)	117 (11%)	
Stage IV	11 (1%)	7 (0.7%)	
Histological type, n (%)			
IDC	371 (38%)	401 (41%)	0.221
ILC	109 (11.2%)	96 (9.8%)	
ER status, n (%)			
Negative	119 (11.5%)	121 (11.7%)	0.634
Indeterminate	0 (0%)	2 (0.2%)	
Positive	394 (38.1%)	399 (38.6%)	
HER2 status, n (%)			
Negative	272 (37.4%)	286 (39.3%)	0.730
Indeterminate	7 (1%)	5 (0.7%)	
Positive	80 (11%)	77 (10.6%)	
PAM50, n (%)			
Normal	33 (3%)	7 (0.6%)	<0.001
Luminal A	295 (27.2%)	267 (24.7%)	
Luminal B	82 (7.6%)	122 (11.3%)	
Her-2 +	46 (4.2%)	36 (3.3%)	
Basal-like	85 (7.8%)	110 (10.2%)	

Note: IDC, invasive ductal carcinoma; ILC, invasive lobular carcinoma; ER, estrogen receptor; PR, progesterone receptor.

The related genes and signal pathways of CDC73 in breast cancer

In the xiantao platform, we found the differential expression of *CDC73* in breast cancer and built up the volcano map (Fig. 2A). KEGG analysis showed that the top signaling pathway included enzyme inhibitors, peptidases, and keratinization (Fig. 2B, p<0.05). GESA analysis showed that the top signaling pathways composed of ribosomes, TGF-β, oxidation phosphorylation, inositol phosphate metabolism, arachidonic acid metabolism, linoleic acid metabolism, ERBB, and VEGF signaling pathways (Fig. 2C, p<0.05). In addition, STRING was used to identify the PPI network (Fig. 3A) and the cystoscope was used to find the top 10 hub nodes ranked by degree (Fig. 3B). According to the xiantao database, expression of *CASP14, LOR, SPRR2E, LCE3D, SPRR2A, SPRR2B,* and *SPRR2G* were increased in breast cancer compared

Table 2. The correlation between CDC73 mRNA expression and immune cell infiltration in breast cancer.

Cells	CDC73 expression	
	Pearson	P
aDC	-0.076	0.012
B cells	-0.089	0.003
CD8 T cells	-0.249	<0.001
Cytotoxic cells	-0.242	<0.001
DC	-0.187	<0.001
Eosinophils	0.004	0.907
iDC	-0.166	<0.001
Macrophages	0.022	0.458
Mast cells	-0.092	0.002
Neutrophils	-0.083	0.006
NK CD56bright cells	-0.309	<0.001
NK CD56dim cells	-0.184	<0.001
NK cells	-0.258	<0.001
pDC	-0.365	<0.001
T cells	-0.067	0.026
T helper cells	0.373	<0.001
Tcm	0.499	<0.001
Tem	0.010	0.743
TFH	-0.039	0.198
Tgd	0.151	<0.001
Th1 cells	-0.064	0.033
Th17 cells	0.121	<0.001
Th2 cells	0.210	<0.001
Treg	-0.174	<0.001

to normal tissues (Fig. 4C, $p<0.05$).

According to Xiantao database, the positively-correlated genes of CDC73 in breast cancer were shown in the hot map of Fig. 4A ($p<0.05$). Furthermore, it was found that these genes are involved in cell mobility, response to interferon α, nuclear pore and basket, and histone methyltransferase (Fig. 4B). The genes that negatively correlated with *CDC73* in breast cancer are shown in the heat map (Fig. 4C, $p<0.05$), these genes are involved in the mitochondrial respiratory chain, thermogenesis, and ribosomes, to name a few (Fig. 4D). The genes that correlated positively with *CDC73* (*RO60, RBBP5, RAB3GAP2, ZBTB41, CEP350, SDE2, TPR,* and *FBXO28*) showed increased expression in breast cancer compared to normal tissue (Fig. 5, $p<0.05$), but the converse was true for *NEK7*. The expression of some negatively-correlated genes (*AURKAIP1, NDUFB7, GADD45GIP1, ATP5F1D, EDF1, FKBP2, NDUFA13,* and *RPL28*) was higher in breast cancer than in normal tissue (Fig. 6, $p<0.05$). *RO60, RAB3GAP2,* and *FBX028* negatively correlated with OS in breast cancer patients, but *FAU* and *RPL28* correlated positively with OS (Fig. 6, $p<0.05$). There was a negative relationship between DSS and *RAB3GAP2* or *SDE2* (Fig. 6, $p<0.05$).

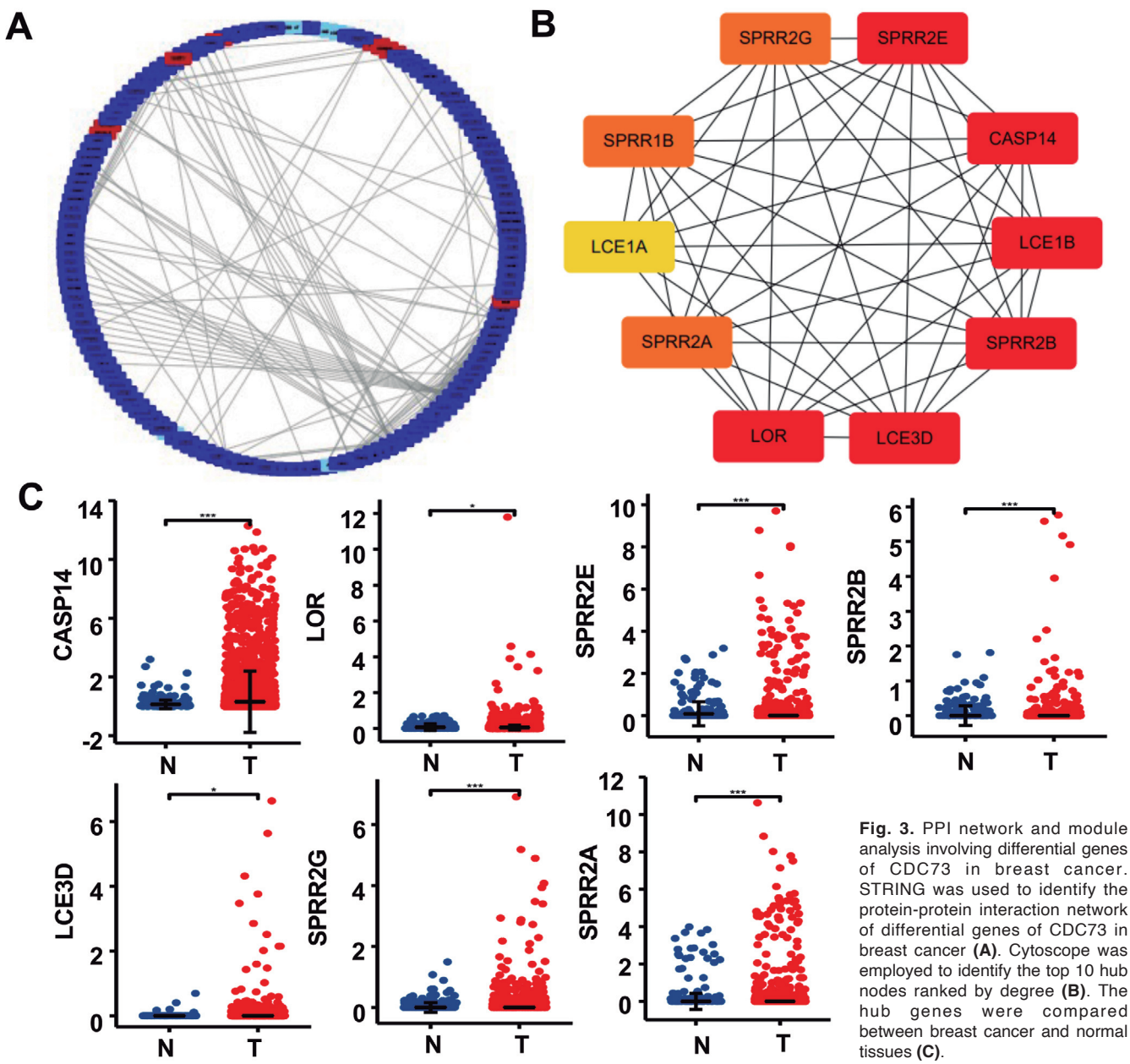

Fig. 3. PPI network and module analysis involving differential genes of CDC73 in breast cancer. STRING was used to identify the protein-protein interaction network of differential genes of CDC73 in breast cancer **(A)**. Cytoscope was employed to identify the top 10 hub nodes ranked by degree **(B)**. The hub genes were compared between breast cancer and normal tissues **(C)**.

RAB3GAP2 and *SDE2* were negatively linked to the PFS, while the converse was true for *FAU, RPL35,* and *RPL28* (Fig. 6, p<0.05).

The correlation of parafibromin expression with carcinogenesis and pathology of breast cancer

According to Western blot analysis, parafibromin expression was higher in breast cancer than in matched normal tissues (Fig. 7A,B, p<0.05), in line with the data from the UALCAN database even when stratified by race and PAM50 subtyping (Fig. 7C-D, p<0.05). Parafibromin expression was higher in T2 and T3 than in T1 breast cancer (p<0.05), invasive ductal than lobular carcinoma (p<0.05), and mucinous adenocarcinoma than others (Fig. 7D, p<0.05).

Immunohistochemistry showed that parafibromin was positively distributed to the nuclei of breast lobular (Fig. 7E) and ductal (Fig. 7F) glands, invasive ductal (Fig. 7G-I) and lobular carcinoma (Fig. 7J-L), embolus cancer cells (Fig. 7M) and metastatic cancer in lymph nodes (Fig. 7N). Parafibromin expression was detectable in normal breast tissue (73.6%, 81/110), primary cancer (83.4%, 549/658), and metastatic cancer in lymph nodes (74.1%, 60/81). Statistically, parafibromin expression was higher in primary cancers than in normal tissue and metastatic cancers (p<0.05, Table 3). Parafibromin expression was not linked to age, T staging, N staging, M staging, TNM staging, histological grading, ER expression, PR expression, Her-2 expression, or ki-67 expression (Table 4, p>0.05). Age and parafibromin expression were independent factors to indicate the favorable prognosis of breast cancer patients (p<0.05, Fig. 7O and Table 5).

Table 3. Parafibromin expression in breast carcinogenesis and subsequent progression.

Groups	n	Parafibromin expression				
		-	+	++	+++	%
Normal breast tissues	110	29	42	31	8	73.6
Primary cancer	658	109	276	172	101	83.4*
Metastatic cancer	81	21	45	11	4	74.1**

%, positive rate; *, compared to normal tissues, p=0.019; **, compared to primary cancer, p<0.001.

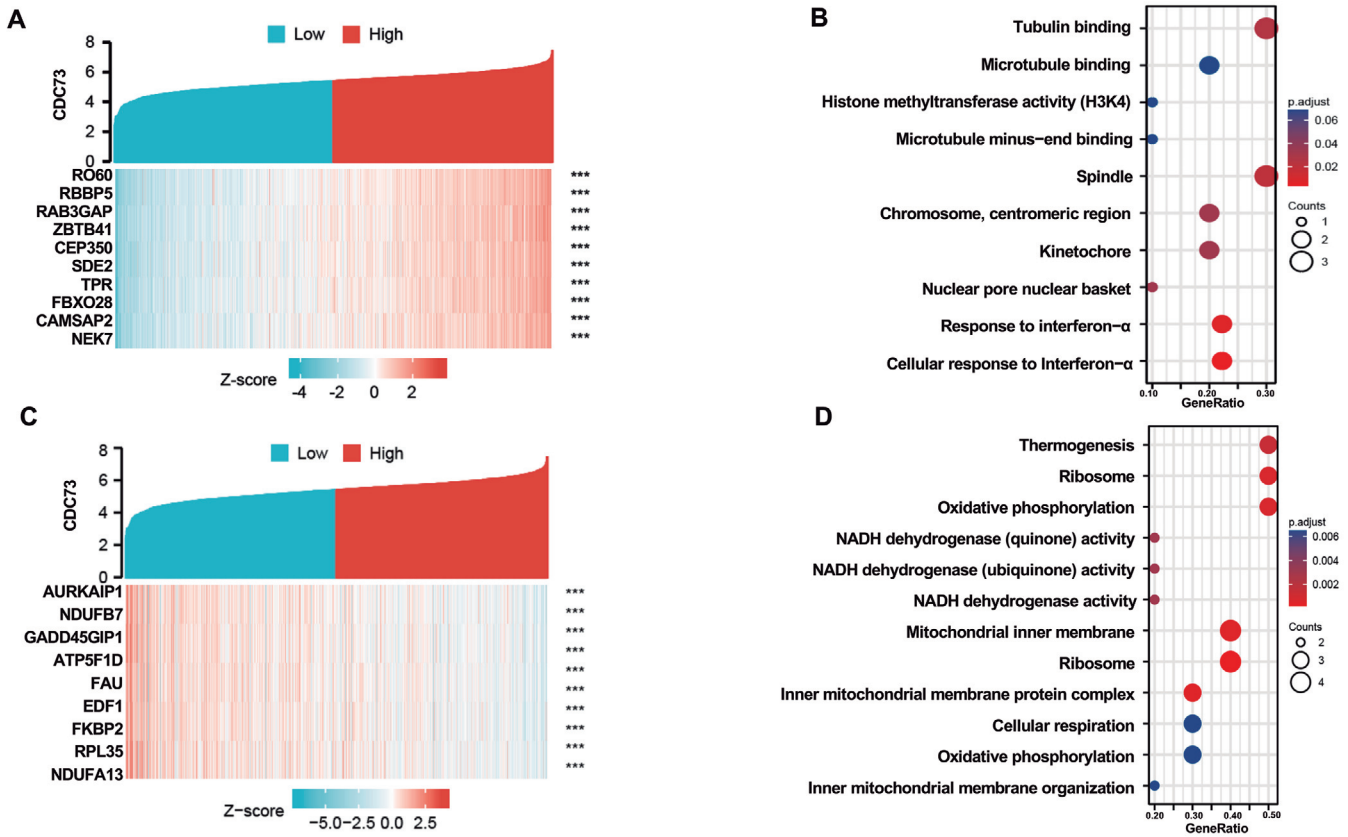

Fig. 4. The CDC73-related genes and signaling pathways in breast cancer. The top positively-related genes of CDC73 were screened according to the hot map **(A)** and were classified into the signaling pathway using the xiantao database **(B)**. The top negatively-related genes of CDC73 were screened according to the hot map **(C)** and were classified into signaling pathways using the xiantao database **(D)**.

Table 4. The relationship between parafibromin expression and clinicopathological characteristics of breast cancer.

Clinicopathological features		Parafibromin expression					
		-	+	++	+++	%	p
Age (years)							0.697
<55	403	66	172	104	61	83.6	
≥55	247	40	101	67	39	83.8	
T staging							0.545
Tis	2	0	0	1	1	100	
1	217	39	90	55	33	82.0	
2	379	62	161	98	58	83.6	
3	34	5	12	11	6	85.3	
4	14	1	8	4	1	92.9	
N staging							0.552
0	368	55	156	98	59	85.1	
1	138	31	54	34	19	77.5	
2	83	16	37	20	10	80.7	
3	59	5	25	19	10	91.5	
M staging							0.539
0	497	83	208	133	73	83.3	
1	13	2	7	3	1	84.6	
TNM Staging							0.372
1	136	17	56	39	24	87.5	
2	337	65	140	83	49	80.7	
3	158	23	70	43	22	85.4	
4	12	1	7	3	1	91.7	
Histological grade							0.075
1	24	2	8	9	5	91.7	
2	412	70	162	116	64	83.0	
3	34	4	20	7	3	88.2	
ER expression							0.208
-	193	30	81	46	36	84.5	
+	128	22	40	36	30	82.8	
++	92	19	34	30	9	79.3	
+++	138	23	60	41	14	83.3	
PR expression							0.360
-	252	41	103	59	49	83.7	
+	155	26	54	51	24	83.2	
++	86	16	34	24	12	81.4	
+++	57	11	23	19	4	80.7	
Her-2 expression							0.759
-	127	18	48	36	25	85.8	
+	167	35	66	41	25	79	
++	182	31	70	55	26	83	
+++	71	10	29	20	12	85.9	
Ki-67							0.573
-	226	44	83	59	40	80.5	
+~+++	112	22	36	30	24	80.4	

ER, estrogen receptor; PR, progesterone receptor.

Table 5. Survival analysis for the breast cancer patients.

Clinicopathological features	Univariate analysis		Multivariate analysis	
	HR (95% CI)	p	HR (95% CI)	p
Age (<55 vs + ≥55, years)	1.360 (1.017-1.817)	0.038	1.640 (1.111-2.420)	0.013
Histological grade (1 vs 2,3)	1.122 (0.842-1.495)	0.433		
T staging (Tis-2 vs T3-4)	1.076 (0.810-1.428)	0.613		
N staging (N0-1 vs N2-3)	1.254 (0.884-1.780)	0.204		
M staging (M0 vs M1)	0.734 (0.390-1.380)	0.337		
TNM staging (I-II vs III-IV)	1.049 (0.764-1.439)	0.786		
ER expression (-~+vs ++~+++)	0.875 (0.573-1.337)	0.538		
PR expression (-~+vs ++~+++)	1.390 (0.818-2.361)	0.224		
Her2 expression (-~+vs ++~+++)	0.931 (0.606-1.428)	0.742		
Ki-67 expression (-~+vs ++~+++)	1.409 (0.803-2.472)	0.232		
Parafibromin expression (-vs +~+++)	0.486 (0.281-0.839)	0.010	0.548 (0.314-0.959)	0.035

HR, hazard ratio; CI, confidence interval; ER, estrogen receptor; PR, progesterone receptor.

Discussion

Bioinformatics analysis indicated that *CDC73* mRNA was overexpressed in gastric, lung, breast, and ovarian cancers. However, RT-PCR showed *CDC73* hypoexpression in colorectal, lung, and ovarian cancers (Zheng et al., 2017), in line with the immunohistochemical results (Agarwal et al., 2008; Zheng et al., 2011; Shen et al., 2016). In the present study, we found parafibromin overexpression in breast cancer at both mRNA and protein levels according to bioinformatics and pathological analysis, indicating that its upregulation might play an essential role in breast carcinogenesis. Therefore, we speculate that the parafibromin expression profile might depend on the type of cancer and molecular levels of mRNA. Additionally, parafibromin expression was decreased in metastatic versus primary breast cancer, indicating that parafibromin-negative breast cancer cells showed an easier metastasis to lymph nodes or that the tumor microenvironment influenced parafibromin expression.

Although parafibromin protein was detectable in the cilium of the epithelium (Xia et al., 2011; Shen et al., 2016), it was observed in the nuclei of the ductal and lobular epithelial and cancer cells. This suggests that nuclear parafibromin overexpression might suppress the aggressiveness of breast cancer cells due to negative feedback. Reportedly, nuclear parafibromin interacts with the human PAF1 complex and RNA polymerase II to elongate the transcription of Cyclin D1, c-Myc, and VEGF (Kikuchi et al., 2016; Lin et al., 2008). In colorectal cancer cells, nuclear parafibromin was found to suppress proliferation and tumor growth, induction of apoptosis, and cell cycle arrest,; interestingly, it was the opposite for cytosolic parafibromin (Zheng et al., 2017b). Additionally, proteomic alteration could influence the suppressor functions of parafibromin in breast cancer cells.

In a previous study, we found that *CDC73* mRNA expression was higher in gastrointestinal-type than diffuse-type carcinomas and positively linked to distant metastasis and clinicopathological stage of lung cancer (Zheng et al., 2017a). Parafibromin expression was negatively linked to T stage, N stage, TNM stage of laryngeal squamous cell carcinoma (Cho et al., 2016), HNSCC (Zhang et al., 2015), urothelial carcinoma (Karaarslan et al., 2015), gastric, and colorectal cancer. Selvarajan et al. found that parafibromin expression negatively correlated with T stage, clinicopathological stage, local lymphovascular invasion, and C-erbB2 expression in breast cancer, which is the opposite of our bioinformatics findings (Selvarajan et al., 2008). The discrepancy might be attributable to our usage of TMA and the difference in the processing of the methods. Additionally, *CDC73* mRNA expression is positively correlated with HPV-related HNSCC, in line with the immunohistochemical result (Zhang et al., 2015). It is suggested that parafibromin expression might be

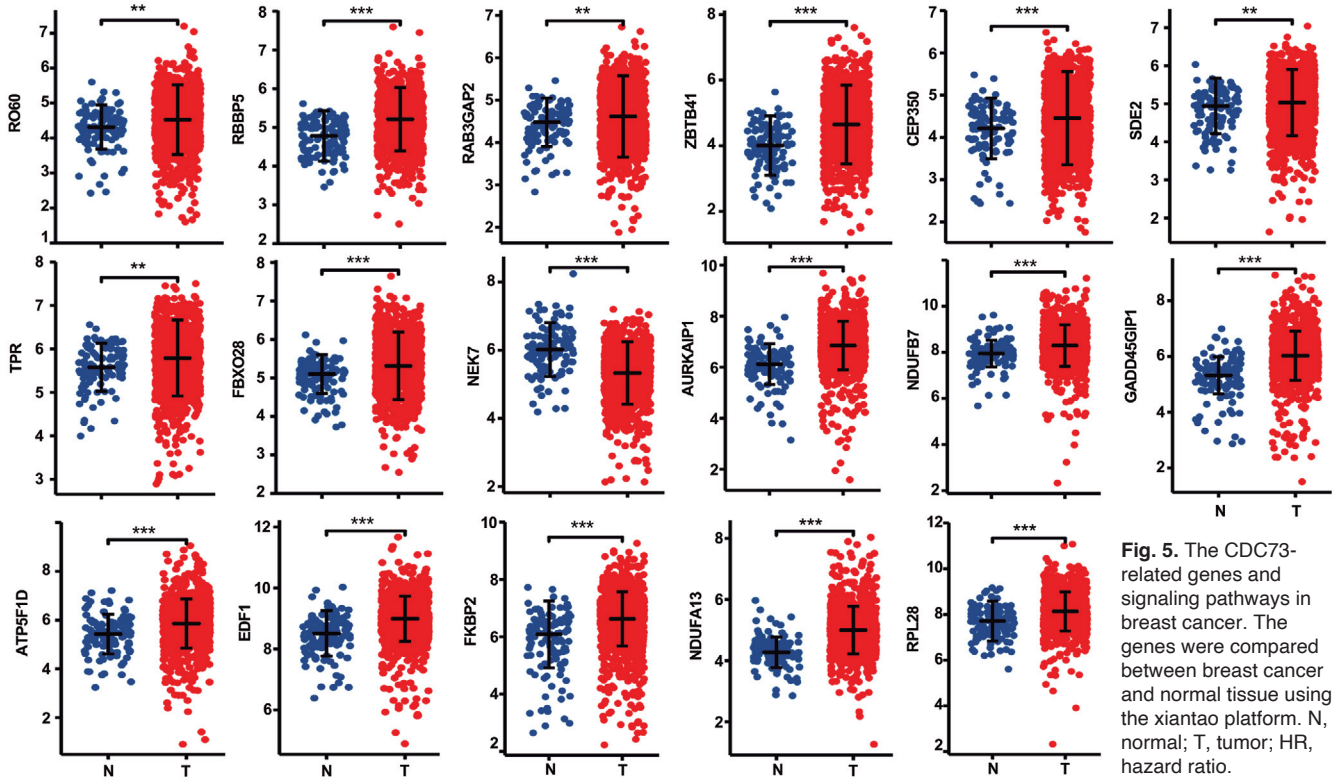

Fig. 5. The CDC73-related genes and signaling pathways in breast cancer. The genes were compared between breast cancer and normal tissue using the xiantao platform. N, normal; T, tumor; HR, hazard ratio.

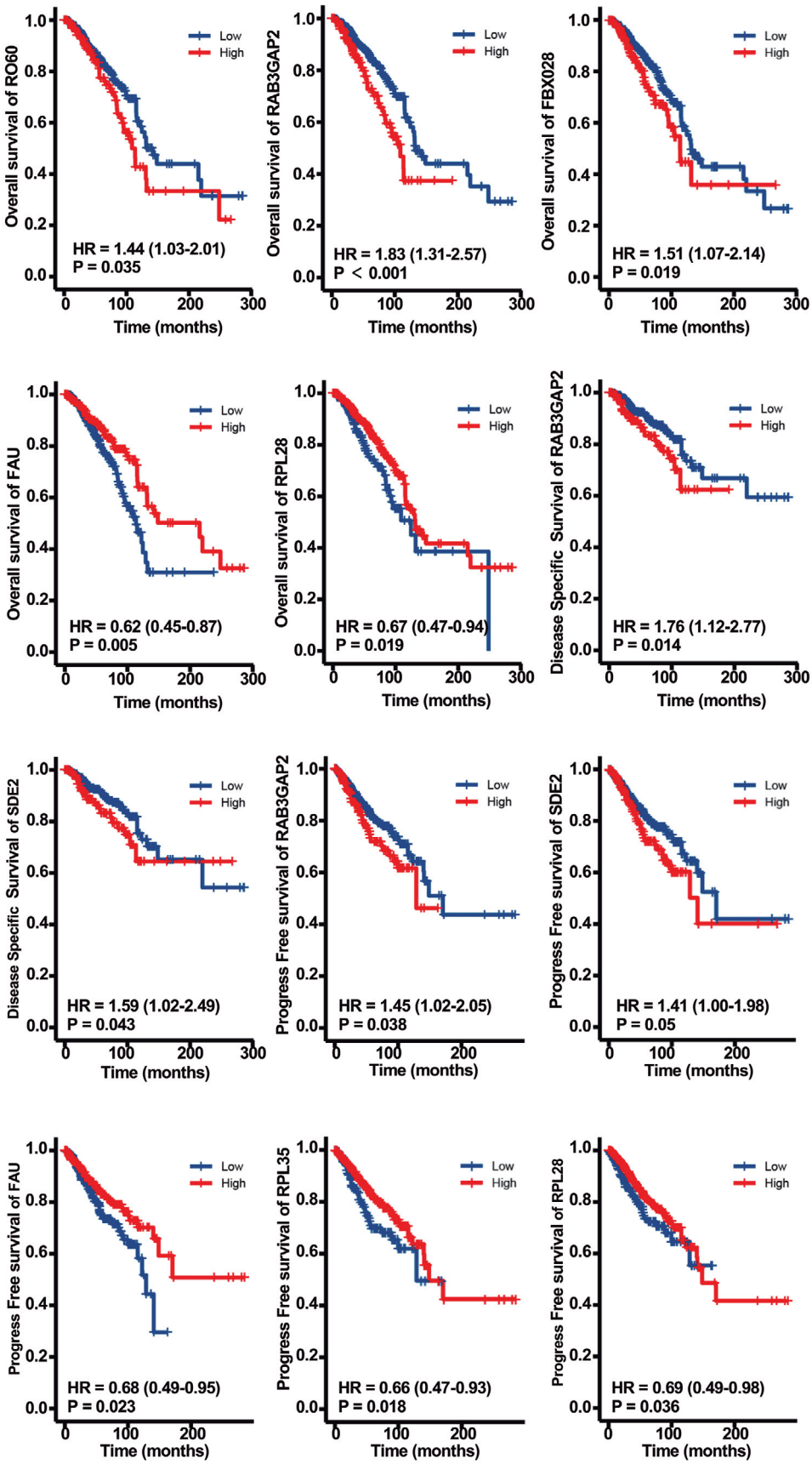

Fig. 6. The CDC73-related genes and signaling pathways in breast cancer. The expression differences of genes correlated to the overall (OS), disease-specific (DSS), and progression-free (PFS) survival of the breast cancer patients .

involved in HPV infection of the head and neck region.

Histologically, parafibromin expression was higher in invasive ductal than lobular carcinoma, indicating that it might be involved in the histogenesis of breast cancer. According to PAM50 subtypes of breast cancer, *CDC73* mRNA was preferably expressed in luminal subtypes, indicating that *CDC73* might be employed to identify favorable PAM50 subtypes. In 2011, Lehmann et al. classified triple-negative breast cancer (TNBC) into basal-like (BL1, BL2), immunomodulatory (IM), mesenchymal (M), mesenchymal stem-like (MSL), and luminal androgen receptor (LAR) subtypes (Lehmann et al., 2011). These *PTEN*-low/miRNA-low lesions cluster with BL1 TNBC, while *AKT1* copy gain/high mRNA expression with BL2 TNBC (Wang et al., 2019). The higher *CDC73* expression in BL1 compared to the BL2 subtype also underlay the molecular basis for both groups. The negative relationship between *CDC73* expression and immune infiltration might be responsible for higher parafibromin levels seen in TNBC-M compared to -IM patients because IM subtypes had frequent immune cell infiltration.

It has previously been shown that nuclear parafibromin transcription suppresses PI3K-Akt and

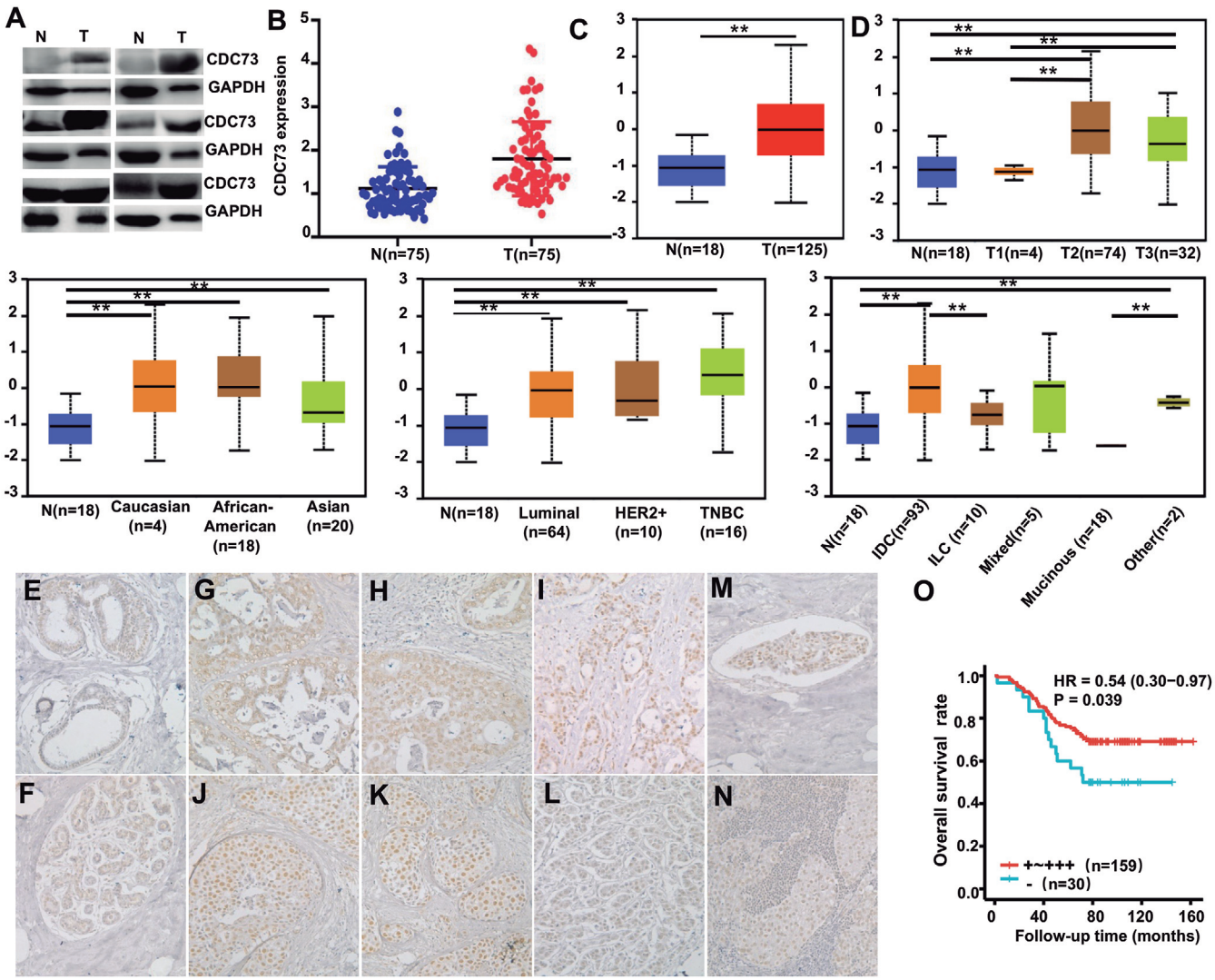

Fig. 7. The clinicopathological significance of parafibromin protein expression in breast cancer. Western blot analysis was used to detect parafibromin protein levels in breast cancer **(A)**. Densitometry analysis showed higher expression in breast cancer than in normal tissues (**B**, $p<0.05$), in agreement with the result from UALCAN (**C**, $p<0.05$). Parafibromin protein expression was compared with the clinicopathological characteristics of breast cancer **(D)**. Immunohistochemically, parafibromin protein was positively expressed in the nuclei of ductal **(E)** and lobular **(F)** epithelial cells and ductal **(G-I)** and lobular **(J-L)** adenocarcinoma. Parafibromin was observed in the nuclei of embolus cancer cells within lymphatic vessels **(M)** and metastatic cancer cells in lymph nodes **(N)**. There was a positive relationship between parafibromin expression and the overall survival of breast cancer patients **(O)**. N, normal; T, tumor; HR, hazard ratio; IDC, invasive ductal carcinoma; ILC, invasive lobular carcinoma.

FoxO signaling pathways, while cytosolic parafibromin activates the PI3K-Akt pathway, promote actin-mediated mobility (Zheng et al., 2017b). Here, we found that differential genes of *CDC73* were involved in peptidase and its inhibitor, keratinization, ribosomes, TGF-β, oxidation phosphorylation, fatty acid metabolism, and inositol phosphate. The *CDC73*-correlated genes were involved in cell mobility, histone methyltransferase, mitochondrial respiratory chain, and ribosomes. These bioinformatics findings indicate that CDC73 might regulate biological processes, including ribosomes, mitochondrial oxidation, gene transcription, and cell mobility in breast cancer.

According to immunohistochemistry, parafibromin expression is negatively correlated with poor prognosis of gastric (Zheng et al., 2008), colorectal (Zheng et al., 2011), ovarian (Xia et al., 2011), and HNSCC (Zhang et al., 2015). Furthermore, parafibromin was an independent protective factor of colorectal (Zheng et al., 2011) and HNSCC (Zhang et al., 2015). Bioinformatics analysis showed that CDC73 mRNA expression positively correlates with OS and PFS in gastric cancer patients, even when stratified by gender, lymph node involvement, or treatment. The opposite is true in breast cancer patients (Zheng et al., 2017a). In our study, both pathological and bioinformatics analyses indicated that the mRNA and protein expression of *CDC73* was positively linked to a favorable prognosis of breast cancer, including OS, PFS, and PPS. Combined, these results suggest that *CDC73* overexpression might be involved in improved prognosis for breast cancer patients.

In conclusion, parafibromin expression contributed to tumorigenesis, histological, and molecular subtyping of breast cancer by regulating metabolism, mitochondrial oxidation, ribosomes, and cytokines. It was closely linked to a favorable prognosis for breast cancer patients.

Acknowledgements. The present study was supported by the Award for Liaoning Distinguished Professor, Natural Science Foundation of Hebei Province (21377772D; H2022406034), and the National Natural Scientific Foundation of China (81672700).

Competing interest. The authors declare that they have no competing interests.

References

Agarwal S.K., Simonds W.F. and Marx S.J. (2008). The parafibromin tumor suppressor protein interacts with actin-binding proteins actinin-2 and actinin-3. Mol. Cancer 7, 65.

Aldred M.J., Talacko A.A., Savarirayan R., Murdolo V., Mills A.E., Radden B.G., Alimov A., Villablanca A. and Larsson C. (2006). Dental findings in a family with hyperparathyroidism-jaw tumour syndrome and a novel HRPT2 gene mutation. Oral. Surg. Oral. Med. Oral. Pathol. Oral. Radiol. Endod. 101, 212- 218.

Cho I., Lee M., Lim S. and Hong R. (2016). Significance of Parafibromin expression in laryngeal squamous cell carcinomas. J. Pathol. Transl. Med. 50, 264-269.

Coughlin S.S. (2019). Epidemiology of breast cancer in women. Adv. Exp. Med. Biol. 1152, 9-29.

Hahn M.A., Dickson K.A., Jackson S., Clarkson A., Gill A.J. and Marsh D.J. (2012). The tumor suppressor CDC73 interacts with the ring finger proteins RNF20 and RNF40 and is required for the maintenance of histone 2B monoubiquitination. Hum. Mol. Genet. 21, 559-568.

Karaarslan S., Yaman B., Ozturk H. and Kumbaraci B.S. (2015). Parafibromin staining characteristics in urothelial carcinomas and relationship with prognostic parameters. J. Pathol. Transl. Med. 49, 389-395.

Kikuchi I., Takahashi-Kanemitsu A., Sakiyama N., Tang C., Tang PJ., Noda S., Nakao K., Kassai H., Sato T., Aiba A. and Hatakeyama M. (2016). Dephosphorylated parafibromin is a transcriptional coactivator of the Wnt/Hedgehog/Notch pathways. Nat. Commun. 7, 12887.

Lehmann B.D., Bauer J.A., Chen X., Sanders M.E., Chakravarthy A.B., Shyr Y. and Pietenpol J.A. (2011). Identification of human triple-negative breast cancer subtypes and preclinical models for selection of targeted therapies. J. Clin. Invest. 12, 2750-2767.

Lin L., Zhang J.H., Panicker L.M. and Simonds W.F. (2008).The parafibromin tumor suppressor protein inhibits cell proliferation by repression of the c-myc proto-oncogene. Proc. Natl. Acad. Sci. USA 105, 17420-17425.

Nene R.V., Putnam C.D., Li B.Z., Nguyen K.G., Srivatsan A., Campbell C.S., Desai A. and Kolodner R.D. (2018). Cdc73 suppresses genome instability by mediating telomere homeostasis. PLoS Genet. 14, e1007170.

Pyo J.S. and Cho W.J. (2019). Diagnostic and prognostic implications of parafibromin immunohistochemistry in parathyroid carcinoma. Biosci. Rep. 39, BSR20181778.

Rojas K. and Stuckey A.(2016). Breast cancer epidemiology and risk factors. Clin. Obstet. Gynecol. 59, 651-672.

Selvarajan S., Sii L.H., Lee A., Yip G., Bay B.H., Tan M.H., Teh B.T. and Tan P.H. (2008). Parafibromin expression in breast cancer: a novel marker for prognostication? J. Clin. Pathol. 61, 64-67.

Shen D.F., Liu X., Yang X.F., Fang L., Gao Y., Zhao S., Wu J.C., Shi S., Li J.J., Zhao X.X., Gou W.F. and Zheng H.C. (2016). The roles of parafibromin expression in ovarian epithelial carcinomas: a marker for differentiation and prognosis and a target for gene therapy. Tumour Biol. 37, 2909-2924.

Takahashi A., Tsutsumi R., Kikuchi I., Obuse C., Saito Y., Seidi A., Karisch R., Fernandez M., Cho T., Ohnishi N., Rozenblatt-Rosen O., Meyerson M., Neel B.G. and Hatakeyama M. (2011). SHP2 tyrosine phosphatase converts parafibromin/Cdc73 from a tumor suppressor to an oncogenic driver. Mol. Cell. 43, 45-56.

Walls G.V., Stevenson M., Lines K.E., Newey P.J., Reed A.A.C., Bowl M.R., Jeyabalan J., Harding B., Bradley K.J., Manek S., Chen J., Wang P., Williams B.O., Teh B.T. and Thakker R.V. (2017). Mice deleted for cell division cycle 73 gene develop parathyroid and uterine tumours: model for the hyperparathyroidism-jaw tumour syndrome. Oncogene 36, 4025-4036.

Wang D.Y., Jiang Z., Ben-David Y., Woodgett J.R. and Zacksenhaus E. (2019). Molecular stratification within triple-negative breast cancer subtypes. Sci. Rep. 9, 19107.

Wei J., Lian H., Zhong B. And Shu H.B. (2015). Parafibromin is a component of IFN-γ- triggered signaling pathways that facilitates JAK1/2-mediated tyrosine phosphorylation of STAT1. J. Immunol.

195, 2870-2878.

Witteveen J.E., Hamdy N.A., Dekkers O.M., Kievit J., van Wezel T., Teh B.T., Romijn J.A. and Morreau H. (2011). Downregulation of CASR expression and global loss of parafibromin staining are strong negative determinants of prognosis in parathyroid carcinoma. Mod. Pathol. 24, 688-697.

Xia P., Wang W., Xu X.Y., Wang J.P., Takano Y. and Zheng H.C. (2011). Parafibromin expression in lung normal tissue and carcinoma: its comparison with clinicopathological parameters of carcinoma. Histol. Histopathol. 26, 1039-1047.

Yang Y.J., Han J.W., Youn H.D. and Cho E.J. (2010). The tumor suppressor, parafibromin, mediates histone H3K9 methylation for cyclin D1 repression. Nucleic. Acids. Res. 38, 382-390.

Zhang Z., Yang X.F., Huang K.Q., Ren L., Gou W.F., Shen D.F., Zhao S., Sun H.Z., Takano Y. and Zheng H.C. (2015). The clinicopathological significances and biological functions of parafibromin expression in head and neck squamous cell carcinomas. Tumor. Biol. 36, 9487-9497.

Zheng H.C., Takahashi H., Li X.H., Hara T., Masuda S., Guan Y.F. and Takano Y. (2008). Downregulated parafibromin expression is a promising marker for pathogenesis, invasion, metastasis and prognosis of gastric carcinomas. Virchows Arch. 452, 147-155.

Zheng H.C., Wei Z.L., Xu X.Y., Nie X.C., Yang X., Takahashi H. and Takano Y. (2011). Parafibromin expression is an independent prognostic factor for colorectal carcinomas. Hum. Pathol. 42,1089-1102.

Zheng H.C., Gong B.C. and Zhao S. (2017a). The clinicopathological and prognostic significances of CDC73 expression in cancers: a bioinformatics analysis. Oncotarget 8, 95270-95279.

Zheng H.C., Liu J.J., Li J., Wu J.C., Yang L., Zhao G.F., Zhao X., Jiang H.M., Huang K.Q. and Li Z.J. (2017b). The *in vitro* and *in vivo* effects of nuclear and cytosolic parafibromin expression on the aggressive phenotypes of colorectal cancer cells: a search of potential gene therapy target. Oncotarget 8, 23603-23612.

Zhu J.J., Cui Y., Cui K., Li X. and Zhang Z.Y. (2016). Distinct roles of parafibromin in the extracellular environment, cytoplasm and nucleus of osteosarcoma cells. Am. J. Transl. Res. 8, 2426-2431.

Zhu R., Wang Z. and Hu Y. (2020). Prognostic role of parafibromin staining and CDC73 mutation in patients with parathyroid carcinoma: a systematic review and meta-analysis based on individual patient data. Clin. Endocrinol. (Oxf). 92, 295-302.

Accepted October 18, 2022